The yellow ink that has transferred to the paper.

The red plate to overprint the paper to reveal the red top print on the yellow

The second: The main drawing of the image is attached to the drawing board with adhesive tape, and it is necessary to reverse if the final print is required to be the same as the original drawing. Prepare 3 pieces of plastic cut to the same size glued on the drawing [3, tr.373].

Step 2: Brush ink color onto 3 plastic sheets

- The fist plastic sheet has been coated with a thin yellow layer, enough to easily reveal the sketch underneath. The ink is removed with wipes, cotton swabs, brushes... to create an array and ready for printing [3, tr.373].

- The second color is bright red which is rolled over the plastic sheet and produces the same print as the previous yellow color [3, tr.373].

- The third and final plastic sheet is rolled color with cyan ink, and shaped similarly to the above 2 colors with rags, paper towels, cotton swabs and brushes. Removed ink sections will produce empty arrays in the final print or will allow color to show up from the next two prints [3, tr.374].

Step 3: Print for monotype

- The moistened printing paper is carefully placed on top of the first plastic sheet, making sure to place the corner of the paper into the corner of the plastic sheet. Printing works best if there are two people to support each other [3, tr.374].

- The print and paper are rolled through the printer, then lifted up to reveal the gold ink that has transferred to the paper. Now you can remove the yellow plastic [3, tr.374].

- The red plate is folded next to overprint the paper to reveal the red top print on the yellow [3, tr.375].

- Finally, cyan plastic sheets are printed in the same way through a press. The cyan acetate plate is removed to reveal the finished print [3, tr.375].

There will be enough ink left on the plastic sheets to print them a second time, in the same order, on a freshly moistened sheet of craft paper. This will create a paler print, so it still be a standalone work because it cannot be the same as the first print. The second print should be done immediately after printing while the ink is still moist, which can do best with Akua's release agent. All prints after drying the ink must be pressed under the boards to flatten the printing.

Note:

- Captioning conventions in prints: The international convention on prints is as follows: note in pencil a horizontal

Finally, The cyan acetate plate is removed to reveal the finished print

The first monoprint

The second print

line, straight along the edges of the left and right edges of the monotype, items in order: number of prints (1/1 means yes only 1 print) material (monotype) size (..cm) title of monotype ("...") name and signature of artist and year of creation.

- Method of preserving and preserving the work: Storing in a closed room with an air conditioning system and a dehumidifier stable at 20-25 degrees (to prevent mold). After the printed dries, it should be placed in a frame glass (to prevent insect invasion) and hang it on the wall - a wall that is not exposed to direct sunlight or rain, is not an outside wall of

(xem tiếp trang 41)

Reflection, transmission of QP- wave at an imperfect interface between two transversly isotropic elastic half-spaces

Do Xuan Tung [1]

Abstract

This work is concerned with the reflection and transmission of quasi-P wave incident at an imperfect interface between two transversely isotropic elastic half-spaces. First, the characteristic equation in the transversely isotropic halfspace is derived. The form of the incident, reflected, and transmitted waves are given. The linear spring model is used to describe the imperfection of bonding behavior at the interface. Then, from the interface conditions for two cases (perfect and imperfect interface), the displacement and stress are required to be satisfied. Reflection, transmission coefficients (RTC) have been derived analytically for when a longitudinal displacement wave strikes an imperfect interface. Finally, numerical examples are provided to show the effect of the imperfect interface and incident angle on the reflection and transmission coefficients.

Key words: reflection, transmission, imperfect interface, transversely isotropic

[1] Assoc.Prof.Dr, Lecturer, faculty of civil engineering, Hanoi Architectural University,
Email: <Tungdx@hau.edu.vn>
Tel: 0984468136

Date of receipt: 25/9/2024
Editing date: 4/11/2024
Post approval date: 04/11/2024

1. Introduction

Reflection and transmission of a plane wave at the interface between two dissimilar media is a fundamental topic in many fields such as seismology, geophysics, earthquake engineering, nondestructive evaluation. As we know, when any of two dissimilar materials are bonded together, the interface cannot be perfectly bonded (imperfect interface) owing to various causes such as micro inhomogeneities, micro defects, micro debonding, etc. To the knowledge of the author, two models are usually proposed to describe the imperfect interface between the two solids. The one is spring model which is analyzed by Hashin [1]. In this model, the properties of the imperfect interface between the two solids can be characterized by the normal and tangential interfacial stiffnesses. The other is membrane model that is formulated by Rokhlin et al. [2]. A thin layer between two solids, where the thickness of the layer ($h \to 0$) denotes a certain magnitude related to imperfect equilibrium at the interface. The imperfect interface considered in these problems means that the stress components are continuous and small dis placement field is not. The values of the interface parameters depend upon the material properties of the medium. More precisely, jumps in the displacement components are assumed to be proportional (in terms of spring-factor-type interface parameters) to their respective interface components. The effects of interfacial imperfection on waves propagating in an isotropic elastic bimaterial have been analyzed by Rokhlin and Wang [2].

Generally speaking, in most of the above investigations, the research works involving the reflection, transmission of waves at imperfect interface have been rare in the published literature so far, to the best knowledge of the authors. Therefore, in this paper, the reflection and transmission problem at imperfect interface between two transversely isotropic elastic half-spaces is considered.

2. Basic equations

We consider homogeneous transversely isotropic elastic medium in such a way that planes of isotropy are perpendicular to x_3-axis. For a two-dimensional problem in which the plane wave is in the plane x_1x_3, the components of strains $\varepsilon_{11}; \varepsilon_{13}; \varepsilon_{33}$ are related to the displacement field $u_1; u_3$ are given by

$$\varepsilon_{11} = u_{1,1}; \varepsilon_{33} = u_{3,3}; \varepsilon_{13} = \varepsilon_{31} = \left(u_{1,3} + u_{3,1}\right)/2 \quad (1)$$

The constitutive relations can be written as [3]

$$\sigma_{11} = c_{11}\varepsilon_{11} + c_{13}\varepsilon_{33}; \sigma_{33} = c_{13}\varepsilon_{11} + c_{33}\varepsilon_{33}; \sigma_{13} = \sigma_{31} = 2c_{44}\varepsilon_{13} \quad (2)$$

where $\sigma_{11}; \sigma_{13}; \sigma_{33}$ are the components of stress tensor and $c_{11}; c_{13}; c_{33}; c_{44}$ are characteristic constants of the transversely isotropic elastic material.

The motion equations in the absence of body force are simplified as [3]

$$\sigma_{11,1} + \sigma_{13,3} = \rho\ddot{u}_1; \sigma_{13,1} + \sigma_{33,3} = \rho\ddot{u}_3 \quad (3)$$

where ρ is the mass density and superposed dot represents the temporal derivative and a comma in the subscript denotes the spatial derivative.

Substituting (2) into (4) and taking into account (1), we obtain the following field equations of a linear transversely isotropic elastic solid, namely

$$c_{11}u_{1,11} + c_{44}u_{1,33} + (c_{13} + c_{44})u_{3,13} = \rho\ddot{u}_1$$

$$(c_{13}+c_{44})u_{1,13}+c_{44}u_{3,11}+c_{33}u_{3,33}=\rho\ddot{u}_3 \quad (4)$$

3. Formulation of the problem

Consider the problem shown in Fig.1. The Ω^+ medium occupies the space Ω^-, which is mechanical bonding with the Ω^- medium occupied the space $x_3<0$: The x_1-axis is taken along the interface and the x_3-axis is directed vertically upwards. For the oblique incidence of the qP wave from the Ω^+ medium at the interface $x_3=0$, all kinds of scattered waves are depicted in Fig.1. The transmitted wave fields consist of the transmitted qP, qSV waves. The reflected wave fields include the reflected qP, qSV waves.

The plane wave solutions of (4) in $x_1\,x_3$ plane is of the form [4,5]

$$u_1=a_1e^{ik(x_1+\xi x_3-ct)};u_3=a_3e^{ik(x_1+\xi x_3-ct)} \quad (5)$$

where k is the x_1-component of the wavenumber, c is phase velocity along x_1, ξ is an unknown ratio of the wave vector components along the x_1- and x_1-directions, a_1, a_3 are unknown amplitudes of the displacement. The generalized Snell's law has been taken into account in (5).

Substituting (5) into (4) yields a system equation in two unknowns a_1, a_3. The determinant of the corresponding coefficients, which yields a characteristic equation

$$t_4\xi^4-t_2\xi^2+t_0=0 \quad (6)$$

where

$$t_4=c_{33}c_{44};$$

$$t_2=c_{13}^2-c_{11}c_{33}+2c_{13}c_{44}+(c_{33}+c_{44})\rho c^2;$$

$$t_0=(c_{44}-\rho c^2)(c_{11}-\rho c^2)$$

Equation (6) has two solutions for ξ^2, each of which represents a pair of partial waves. These waves are quasi-pressure (qP), quasi-shear vertical (qSV) propagating in an opposite direction in each medium.

3.1. Solutions for the upper and lower half-spaces

Equation (6) is quadratic equation in ξ^2 for Ω^+ and Ω^-: We order ξ_n, in such that ξ_1, ξ_2 are positive and ξ_3, ξ_4 are negative correspond to reflected and transmitted waves traveling in the Ω^+, Ω^-, respectively.

- For incident wave:

$$u_1^0=a_0e^{ik(x_1+\xi_0x_3-ct)};u_3^0=a_0w_0e^{ik(x_1+\xi_0x_3-ct)} \quad (7)$$

- For reflected waves:

$$u_1^1=a_1e^{ik(x_1+\xi_1x_3-ct)};u_3^1=a_1w_1e^{ik(x_1+\xi_1x_3-ct)}$$

$$u_1^2=a_2e^{ik(x_1+\xi_2x_3-ct)};u_3^2=a_2w_2e^{ik(x_1+\xi_2x_3-ct)} \quad (8)$$

- For transmitted waves:

$$u_1^3=a_3e^{ik(x_1+\xi_3x_3-ct)};u_3^3=a_3w_3e^{ik(x_1+\xi_3x_3-ct)}$$

$$u_1^4=a_4e^{ik(x_1+\xi_4x_3-ct)};u_3^4=a_4w_4e^{ik(x_1+\xi_4x_3-ct)} \quad (9)$$

where a_i are the amplitudes of the displacement, $w_i=u_3^i/u_1^i$ are the wave amplitude ratios that determined by

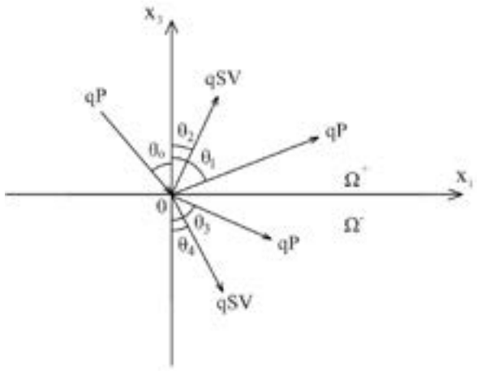

Figure 1. Geometry of problem

$$\sigma_{13}=c_{44}(w+\xi);\sigma_{33}=c_{13}+c_{33}w\xi$$

correspond to the incident, reflected, transmitted waves. In order to consider the boundary conditions in later, we give the components of stresses

$$\sigma_{13}=c_{44}(w+\xi);\sigma_{33}=c_{13}+c_{33}w\xi \quad (10)$$

3.2. Boundary conditions of imperfect interface

The boundary conditions depend on the quality of the interface and involve the normal, tangential displacements and the normal, tangential stresses. The spring model is introduced. At the imperfect interface the normal and tangential stiffness are represented by k_N and k_T, respectively. For finite values of k_N and k_T, the interface behaves as imperfect bonding or weak interface, which can be expressed by [1,6].

$$\sigma_{13}^+=\sigma_{13}^-=k_T(u_1^+-u_1^-);$$

$$\sigma_{33}^+=\sigma_{33}^-=k_N(u_3^+-u_3^-) \quad (11)$$

where

$\sigma_{ij}^+(\sigma_{ij}^-);u_i^+(u_i^-)$ are the fields of stress, displacement of $\Omega^+(\Omega^-)$.

When the stiffness parameters $k_N;k_T\to\infty$ the interface between the two half-spaces is completely perfect. In the case of slip interface, the tangential force along the interface is not supported by the interface. Displacements and normal stresses are continuous but tangential stresses vanish i.e. $k_N\to\infty;k_T\to 0$ [6].

4. The reflection, transmission coefficients

Substituting the quantities of the incident, reflected and transmitted wave field equations (7–9) and the components of stresses (10) into the imperfect mechanical bonding (11), we obtain the following four linear equations about the amplitudes of the reflected and transmitted waves. These equations are expressed as

$$-c_{44}^+(w_1+\xi_1)a_1-c_{44}^+(w_2+\xi_2)a_2+c_{44}^-(w_3+\xi_3)a_3$$
$$+c_{44}^-(w_4+\xi_4)a_4=c_{44}^+(w_0+\xi_0)a_0$$

$$-(c_{13}^++c_{33}^+w_1\xi_1)a_1-(c_{13}^++c_{33}^+w_2\xi_2)a_2$$
$$+(c_{13}^-+c_{33}^-w_3\xi_3)a_3+(c_{13}^-+c_{33}^-w_4\xi_4)a_4$$
$$=(c_{13}^++c_{33}^+w_0\xi_0)a_0$$

$$\left(ic_{44}^+(w_1+\xi_1)-k_T/k\right)a_1+\left(ic_{44}^+(w_2+\xi_2)-k_T/k\right)a_2$$
$$+(k_T/k)a_3+(k_T/k)a_4=\left(ic_{44}^+(w_0+\xi_0)-k_T/k\right)a_0$$

$$\left((c_{13}^++c_{33}^+w_1\xi_1)i-w_1k_N/k\right)a_1$$
$$+\left((c_{13}^++c_{33}^+w_2\xi_2)i-w_2k_N/k\right)a_2$$
$$+(w_3k_N/k)a_3+(w_4k_N/k)a_4$$
$$=\left((c_{13}^++c_{33}^+w_0\xi_0)i-w_0k_N/k\right)a_0 \quad (12)$$

Denoting $A_1=a_1/a_0;A_2=a_2/a_0;$
$A_3=a_3/a_0;A_4=a_4/a_0$

The reflection, transmission coefficients (RTC) are defined by the ratio of the reflected/ transmitted amplitudes to the incident amplitude.

$$R_1=A_1\sqrt{1+w_1^2}/\sqrt{1+w_0^2};$$
$$R_2=A_2\sqrt{1+w_2^2}/\sqrt{1+w_0^2}$$
$$T_1=A_3\sqrt{1+w_3^2}/\sqrt{1+w_0^2}; \quad (13)$$
$$T_2=A_4\sqrt{1+w_4^2}/\sqrt{1+w_0^2}$$

5. Numerical example and discussion

To illustrate the theoretical results obtained in the preceding sections, the following values of materials are used.

For upper half-space Ω^+- Material constants for AlN [6] are given by

$$c_{11}^+=3.45*10^{11}N/m^2;$$
$$c_{13}^+=1.20*10^{11}N/m^2;$$
$$c_{33}^+=3.95*10^{11}N/m^2$$
$$c_{44}^+=1.18*10^{11}N/m^2;$$
$$\rho^+=3.62*10^3kg/m^3$$

For lower half-space Ω^-- Material constants for BaTiO3 [6] are given as

$$c_{11}^-=1.66*10^{11}N/m^2;$$
$$c_{13}^-=0.17*10^{11}N/m^2;$$
$$c_{33}^-=1.62*10^{11}N/m^2$$
$$c_{44}^-=0.453*10^{11}N/m^2;$$
$$\rho^+=5.8*10^3kg/m^3$$

Moreover, to analyze separately the influence of each boundary condition, the tangential and normal spring constants are such that $k_T=2.0;$ $k_N=1.2$ in the first case (imperfect interface). In the second case (perfect interface), $k_T=2^{100};$ $k_N=12^{100}$: For the slip interface, $k_T=0;$ $k_N=12^{100}$.

Fig.2 illustrates the influence of imperfect and perfect interface on RTC with the increasing incident angle θ_0. It can be seen from Figure 2 that the reflection coefficients of qSV (R1) wave and qP (R2) wave (with $\theta_0<58^o$) are quite bigger than the ones in the imperfect, perfect interface, respectively. While the transmission coefficients of qP, qSV for the imperfect interface are quite smaller than the ones for the perfect interface. This shows that the wave passing through the imperfect interface is more difficult than when it passes through perfect interface.

Fig.3 depicts the variation of RTC with the incident angle θ_0 for imperfect and slip interface. In general, in Figure 3,

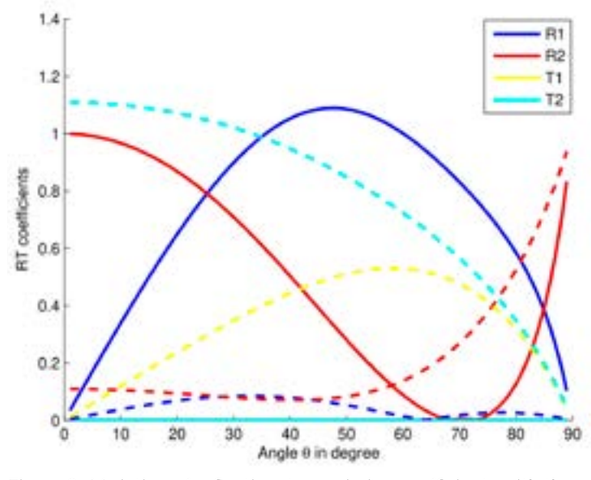

Figure 2. Variation of reflection, transmission coefficients with the incident angle for two cases of boundary conditions: imperfect (solid line) and perfect interface (dashed line)

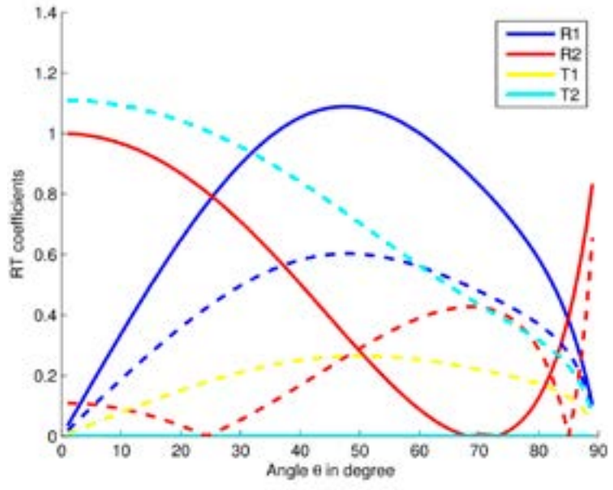

Figure 3. Variation of reflection, transmission coefficients with the incident angle for two cases: imperfect interface (solid line) and slip interface (dashed line).

(xem tiếp trang 56)

due to CFRP debonding. Therefore, it was recommended that the dimensions (i.e., length and width) and layout of the CFRP sheets be carefully considered to obtain the highest strengthening performance.

4. Conclusions

This research investigated the flexural behavior of one-way concrete slabs with openings reinforced with GFRP bars and strengthened using CFRP sheets through NLFE analysis. First, the results suggested that using proper concrete compressive strengths improved the performance of the slab, with better incorporation of CFRP sheets. In this study, the concrete compressive strengths ranging from 30 MPa to 35 MPa were more suitable with the sample's setup. Secondly, it can be observed that increasing the reinforcement ratio reduces ductility while increasing the ultimate strength of the slab sample. The GFRP bars also participated more in the case of a smaller reinforcement ratio. Finally, the disposition layout of CFRP sheets was considered, revealing its influence on the slab's stiffness and ductility. A disposition layout concentrated around the opening improved its performance. Theparametric investigations thus providedvaluable insights into optimizing the structural performance of the considered slabs./.

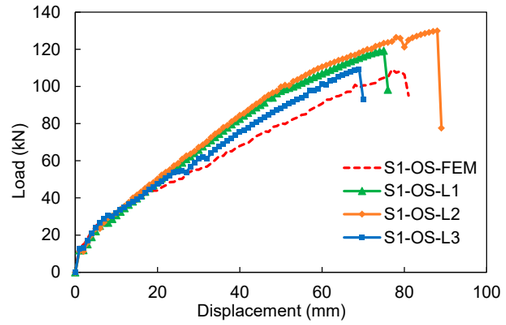

Figure 7. Load-displacement curves of CFRP-strengthened slabs with considered strengthening layouts

References

1. *M. Z. Naser, R. A. Hawileh, and J. A. Abdalla. Fiber-reinforced polymer composites in strengthening reinforced concrete structures: A critical review Engineering Structures, vol. 198, 109542, 2019.*
2. *N. T. Nguyen, T. K. Nguyen, D. H. Du, D. N. Nguyen, and T. S. Kieu.Nonlinear finite element analysis of FRP-strengthened full-size reinforced concrete beams.Innovative Infrastructure Solutions, vol. 8, no. 5, p. 139, 2023.*
3. *Ö. Anil, N. Kaya, and O. Arslan. Strengthening of one-way RC slab with opening using CFRP strips.Construction and Building Materials, vol. 48, 883–893,2013.*
4. *H. M. Afefy and T. M. Fawzy. Strengthening of RC one-way slabs including cut-out using different techniques.Engineering Structures, vol. 57, 23–36,2013.*
5. *T. K. Nguyen, N. T. Nguyen, H. A. Tran, H. G. Nguyen, and P. Tran. Three-dimensional nonlinear finite element analysis of corroded reinforced concrete beams strengthened by CFRP sheets.European Journal of Environmental and Civil Engineering, 1–27, 2024.*
6. *H. D. Vu and D. N. Phan. A framework for predicting the debonding failure modes of RC beams strengthened flexurally with FRP sheets.Innovative Infrastructure Solutions, vol. 7, no. 5, 292, 2022.*
7. *M. A. Golham and A. H. A. Al-Ahmed. Strengthening of GFRP Reinforced Concrete Slabs with Openings.Journal of Engineering, vol. 30, no. 01, 157–172, 2024.*
8. *X. Z. Lu, J. G. Teng, L. P. Ye, and J. J. Jiang. Bond–slip models for FRP sheets/plates bonded to concrete.Engineering Structures, vol. 27, no. 6, 920–937, 2005.*
9. *A. A. Mansor, A. S. Mohammed, and W. D. Salman. Effect of longitudinal steel reinforcement ratio on deflection and ductility in reinforced concrete beams.IOP Conference Series: Materials Science and Engineering, vol. 888, no. 1, 012008, Jul. 2020.*

Reflection, transmission of QP- wave at an imperfect interface...

(tiếp theo trang 37)

the reflection coefficients of waves in an imperfect interface are greater than the ones in slip interface while transmission coefficients are the opposite. For the case of slip interface, the valley value of the reflection coefficient of qP wave is attained at $\theta_0=24^o$; 24^o, while that one is attained at $\theta_0=68^o$; 72^o for imperfect interface.

6. Conclusion

In conclusion, a mathematical study of reflection and transmission coefficients at an imperfect interface separating two transversely isotropic nonlocal elastic solid half spaces is made when longitudinal wave is incident. The three cases of imperfect interfaces are discussed briefly. For the incidence qP wave, the expressions for reflection, transmission coeffi cients of waves in the imperfect/ perfect cases are given. Numerical computations have been performed for a particular model and the results obtained are depicted graphically./.

References

1. *Z. Hashin, The spherical inclusion with imperfect interface. J. Appl. Mech, vol. 58, no. 2, pp. 444–449, 1991.*
2. *S. I. Rokhlin and Y. J. Wang, Analysis of boundary conditions for elastic wave interaction with an inter face between two solids. J. Acoust. Soc. Am, vol. 89, no. 2, pp. 503–515, 1991.*
3. *J. D. Achenbach, Wave Propagation in Elastic Solids. vol. 16. Series in Applied Mechanics. North Holland: Amsterdam. 1973*
4. *A. H. Nayfeh, Wave Propagation in Layered Anisotropic Media, North-Holland: Amsterdam, 1995.*
5. *D. X. Tung, The reflection and transmission of waves at an imperfect interface between two nonlocal transversely isotropic liquid-saturated porous half spaces. Waves Random Complex Media, pp. 1–17, 2021.*
6. *S. Goyal, S. Sahu and S. Mondal, Influence of imperfect bonding on the reflection and transmission of QP-wave at the interface of two functionally graded piezoelectric materials. Wave Motion, vol. 92, pp. 102431, 2020.*

Some safety issues in construction of climbing formwork system in high - rise building construction in Vietnam

Trinh Xuan Vinh[(1)], Tran Tien Huynh[(2)]

Abstract

The paper presents some safety issues in the construction of climbing formwork systems in high-rise building construction in Vietnam.

High-rise buildings impose stringent safety requirements on the implementation of climbing formwork systems. A specific safety plan must be in place, including identifying and eliminating potential hazards, providing adequate personal protective equipment, and ensuring compliance with industry safety regulations and standards.

Safety practices in Vietnam adhere to the national technical standard QCVN 18:2021/BXD on Safety in Construction and draw from international organizations such as OSHA (Occupational Safety and Health Administration of the United States), CEN (European Committee for Standardization), and Japan's guidelines on construction safety regulations. These references provide specific guidance and international standards for the construction of climbing formwork systems.

Key words: Safety; climbing formwork systems; high-rise building

1. Introduction

In the construction industry, the implementation of Climbing formwork systems (CFS) for high-rise buildings requires specialized expertise and particular attention. With high-rise buildings often exceeding 20 floors, safety concerns become increasingly important and need to be carefully considered and addressed.

Figure 1. The Landmark81, Ho Chi Minh City. Source: https://www.coteccons.vn

2. Safety Requirement

High-rise buildings impose stringent safety requirements on the implementation of climbing formwork systems. A specific safety plan must be in place, including identifying and eliminating potential hazards, providing adequate personal protective equipment, and ensuring compliance with industry safety regulations and standards.

Safety practices in Vietnam adhere to the national technical standard QCVN 18:2021/BXD on Safety in Construction and draw from international organizations such as OSHA (Occupational Safety and Health Administration of the United States), CEN (European Committee for Standardization), and Japan's guidelines on construction safety regulations. These references provide specific guidance and international standards for the construction of climbing formwork systems.

In recent years, climbing formwork systems have been widely used in Vietnam due to their ability to meet project schedules, quality requirements, and especially high levels of occupational safety. Safety measures for climbing formwork systems require strict adherence throughout the installation and dismantling processes.

For installation work, the following requirements apply:

- Large formwork panels for multiple levels should only be installed after the formwork for lower levels has been securely fixed.

Msc. Trinh Xuan Vinh
Ha Noi Architectural University
Email: trinhvinh2603@gmail.com,
Tel: 0904330488

Msc. Tran Tien Huynh
Ha Noi Architectural University
Email: trantienhuynhhau@gmail.com,
Tel: 0915666866

Date of receipt:
Editing date:
Post approval date: 03/11/2024